Department of Cardiology[1], First Affiliated Hospital of Nanjing Medical University in Wuxi and People's Hospital of Wuxi City, Wuxi, Department of Cardiology[2], First Affiliated Hospital of Soochow University, Suzhou China

Effects of (*S*)-amlodipine and (*R*)-amlodipine on L-type calcium channel current of rat ventricular myocytes and cytosolic calcium of aortic smooth muscle cells

Ru-xing Wang[1], Wen-ping Jiang[2], Xiao-rong Li[1], Li-hong Lai[2]

Received December 23, 2007, accepted January 11, 2008

Xiao-rong Li, Department of Cardiology, First Affiliated Hospital of Nanjing Medical University in Wuxi and People's Hospital of Wuxi City, 299 Qingyang Road, 214023 Wuxi, China
ruxingw@yahoo.com.cn

Pharmazie 63: 470–474 (2008) *doi: 10.1691/ph.2008.7857*

Objective: Amlodipine (Aml) has *R*- and *S*-isomers with different pharmacological effects. However, no data are available on the influence of (*S*)-Aml and (*R*)-Aml on L-type calcium channel current ($I_{Ca\text{-}L}$) or cytosolic calcium (Ca^{2+}). This study is to investigate effects on $I_{Ca\text{-}L}$ and cytosolic Ca^{2+}. *Methods:* I_{Ca-L}, peak currents, I–V curves, steady state activation curves, steady state inactivation curves and recovery curves from inactivation with (*S*)-Aml and (*R*)-Aml were recorded by whole-cell patch clamp configuration. Cytosolic Ca^{2+} of smooth muscle cells was assayed by Fura-2/AM. *Results:* At the concentrations of 0.1, 0.5, 1, 5, and 10 μmol/L, $1.5 \pm 0.2\%$, $25.4 \pm 5.3\%$, $65.2 \pm 7.3\%$, $78.4 \pm 8.1\%$, and $94.2 \pm 5.0\%$ of I_{Ca-L} were blocked by (*S*)-Aml. I–V curves were shifted upward. Half-activation voltages were -16.01 ± 1.65 mV, -17.61 ± 1.60 mV, -20.17 ± 1.46 mV, -21.87 ± 1.69 mV and -24.09 ± 1.87 mV ($P < 0.05$). Half-inactivation voltages were -27.16 ± 4.48 mV, -28.69 ± 4.52 mV, -31.19 ± 4.17 mV, -32.63 ± 4.34 mV and -35.16 ± 4.46 mV ($P < 0.05$). Recovery time were prolonged gradually ($P < 0.05$). $10.3 \pm 1.2\%$, $35.2 \pm 3.5\%$, $60.1 \pm 5.0\%$, $78.9 \pm 6.1\%$, and $91.2 \pm 7.6\%$ of cytosolic Ca^{2+} were reduced at different concentrations ($P < 0.05$). However, (*R*)-Aml at different concentrations had no effect on I_{Ca-L} and cytosolic Ca^{2+} ($P > 0.05$). *Conclusion:* Only (*S*)-Aml has calcium channel blockade activity, while (*R*)-Aml has none of the pharmacologic actions associated with CCBs.

1. Introduction

Dihydropyridine calcium channel blockers (CCBs) have been proven to be clinically useful in the treatment of hypertension, angina, and certain cardiac arrhythmias (Zanchetti et al. 2006; Sever et al. 2006; Formica et al. 2006). However, all dihydropyridines except nifedipine have a chiral centre, and the pharmacological actions of their isomers are usually different, and even completely opposite (Bojarski 2002; Patil and Kothekar 2006). Amlodipine (Aml) is a dihydropyridine CCB and has two isomers, (*S*)-Aml and (*R*)-Aml, but it is often commercially available as a racemic mixture. Many clinical trials have shown that the racemic mixture has the pharmacological activity associated with CCBs (Zanchetti et al. 2006; Formica et al. 2006; Pathak et al. 2004). However, to our knowledge, there has been no report of cell electrophysiological studies on (*S*)-Aml and (*R*)-Aml, or studies on cytosolic calcium (Ca^{2+}) changes.

To investigate the effects of the different isomers of Aml on L-type calcium channel current (I_{Ca-L}) of rat ventricular myocytes and cytosolic Ca^{2+} changes of aortic smooth muscle cells (SMCs), we studied I_{Ca-L} and its channel kinetics by whole-cell patch clamp configuration, and cytosolic Ca^{2+} changes of SMCs by the fluorescent probe Fura-2/AM. The results may provide experimental evidence for rational applications of different enantiomers of Aml for patients in clinical practice.

2. Investigations and results

2.1. Effects of (S)-Aml and (R)-Aml on I_{Ca-L} and channel kinetic parameters

2.1.1. Effects of (S)-Aml on I_{Ca-L} and channel kinetic parameters

(1) Effects on $I_{Ca\text{-}L}$ and peak currents: The stable baseline peak current was -910.5 ($\pm$ 201.7) pA, and current density was -6.07 (± 1.34) pA/pF ($n = 12$). When (*S*)-Aml was applied at 0.1 μmol/L, 0.5 μmol/L, 1 μmol/L, 5 μmol/L, and 10 μmol/L, I_{Ca-L} of $1.5 \pm 0.2\%$, $25.4 \pm 5.3\%$, $65.2 \pm 7.3\%$, $78.4 \pm 8.1\%$, and $94.2 \pm 5.0\%$ were blocked, respectively ($P < 0.05$, $n = 10$). Figure 1 shows current traces elicited by depolarization from -40 mV HP to 0 mV test potential at the different (*S*)-Aml concentrations. IC_{50} of I_{Ca-L}, calculated by curve fit with concentrations and current blockade percentages, was 0.62 ± 0.12 μmol/L (Fig. 2).

(2) Effects on I–V curves of I_{Ca-L}: When (*S*)-Aml was used at concentrations of 0.1 μmol/L, 0.5 μmol/L, 1 μmol/L, 5 μmol/L, and 10 μmol/L, I_{Ca-L} and current densities were decreased gradually with the increase of (*S*)-Aml concen-

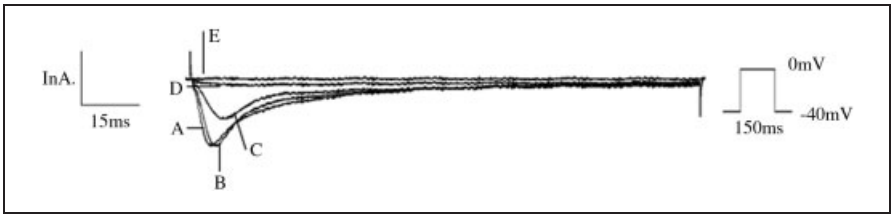

Fig. 1:
I_{Ca-L} blocked by *S*-Aml at different concentrations (A, B, C, D, and E are *S*-Aml at 0, 0.1, 1, 10, and 50 μmol/L, respectively)

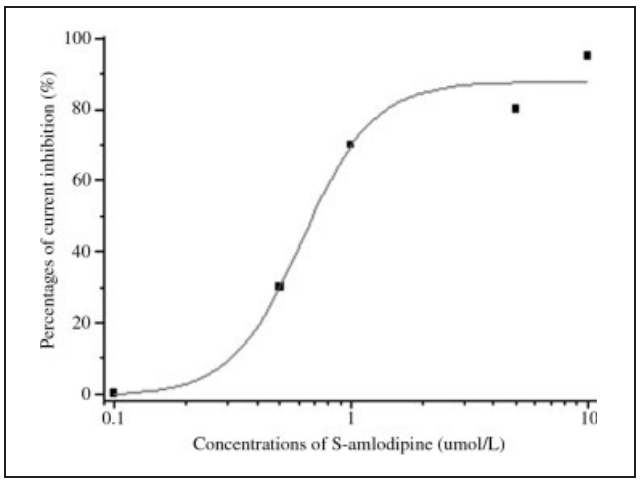

Fig. 2: IC_{50} of I_{Ca-L} blocked by *S*-amlodipine at different concentrations

trations. The I–V curves were shifted upward; however, there was no significant change of morphology, peak current activation potential, threshold potential, or reverse potential (Fig. 3).

(3) Effects on steady-state activation curves of I_{Ca-L}: When 0.1 μmol/L, 0.5 μmol/L, 1 μmol/L, 5 μmol/L, and 10 μmol/L (*S*)-Aml were applied, half-activation voltages were -16.01 ± 1.65 mV, -17.61 ± 1.60 mV, -20.17 ± 1.46 mV, -21.87 ± 1.69 mV, -24.09 ± 1.87 mV, respectively, and slope factors were 5.43 ± 1.42 mV, 5.62 ± 2.01 mV, 5.93 ± 2.21 mV, 6.03 ± 2.32 mV, 6.22 ± 2.43 mV, respectively ($P < 0.05$, $n = 12$). With the increase of (*S*)-Aml concentrations, steady-state activation curves were shifted to the left.

(4) Effects on steady-state inactivation curves of I_{Ca-L}: With (*S*)-Aml concentrations of 0.1 μmol/L, 0.5 μmol/L, 1 μmol/L, 5 μmol/L, and 10 μmol/L, half-inactivation voltages were -27.16 ± 4.48 mV, -28.69 ± 4.52 mV, -31.19 ± 4.17 mV, -32.63 ± 4.34 mV, -35.16 ± 4.46 mV, respectively, and slope factors were -3.53 ± 1.45 mV, -3.50 ± 1.49 mV, -3.38 ± 1.61 mV, -3.17 ± 1.48 mV, -3.01 ± 1.41 mV ($P < 0.05$, $n = 10$). I_{Ca-L} steady-state inactivation curves were shifted to the left with the increase of (*S*)-Aml concentrations.

(5) Effects on I_{Ca-L} recovery curves from inactivation: normal time constant obtained by a single-exponential function fit was 202.3 ± 18.7 ms. With (*S*)-Aml at concentrations of 0.1 μmol/L, 0.5 μmol/L, 1 μmol/L, 5 μmol/L, and 10 μmol/L, time constants were 210.1 ± 19.5 ms, 225.2 ± 21.3 ms, 241.7 ± 2 0.3 ms, 252.3 ± 24.2 ms, and 282.6 ± 23.2 ms, respectively ($P < 0.05$, $n = 10$).

2.1.2. Effects of (R)-Aml on I_{Ca-L} and kinetic parameters

After normal I_{Ca-L}, peak currents, steady-state activation currents, steady-state inactivation currents, and recovery currents from inactivation were recorded; (*R*)-Aml at 0.1 μmol/L, 0.5 μmol/L, 1 μmol/L, 5 μmol/L, and 10 μmol/L was applied, peak currents were -912.4 ± 210.5 pA, -901.3 ± 202.7 pA, -905.7 ± 206.4 pA, -910.4 ± 205.8 pA, -911.7 ± 208.2 pA, and current densities were -6.08 ± 1.40 pA/pF, -6.00 ± 1.35 pA/pF, -6.04 ± 1.38 pA/pF, -6.07 ± 1.37 pA/pF, -6.08 ± 1.39 pA/pF, respectively ($P > 0.05$, $n = 10$). The I–V curves were no change at different concentrations. Half-activation voltages were -14.30 ± 1.11 mV, -14.01 ± 1.30 mV, -13.95 ± 1.17 mV, -14.08 ± 1.22 mV, -14.11 ± 1.20 mV; and slope factors were 5.20 ± 2.14 mV, 5.22 ± 2.00 mV, 5.17 ± 2.01 mV, 5.19 ± 2.02 mV, 5.29 ± 2.23 mV, respectively ($P > 0.05$, $n = 8$). Half-inactivation voltages were -24.4 ± 4.3 mV, -24.0 ± 4.0 mV, -23.9 ± 4.0 mV, -24.7 ± 4.5 mV, -24.5 ± 4.1 mV; and slope factors were -3.55 ± 1.02 mV, -3.60 ± 1.10 mV, -3.51 ± 1.04 mV, -3.61 ± 1.07 mV, -3.47 ± 1.11 mV, respectively ($P > 0.05$, $n = 10$). Time constants of recovery curves from inactivation were 202.1 ± 18.6 ms, 201.4 ± 19.2 ms, 200.9 ± 17.9 ms, 203.5 ± 18.8 ms, and 205.2 ± 19.7 ms, respectively ($P > 0.05$, $n = 8$).

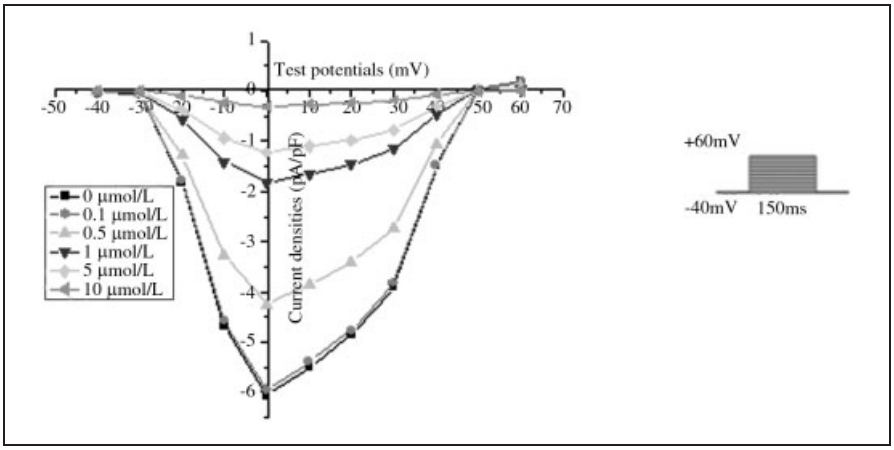

Fig. 3:
I–V curves of I_{Ca-L} blocked by *S*-amlodipine at different concentrations

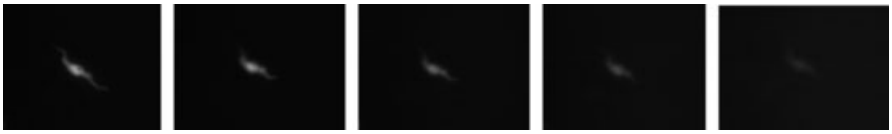

Fig. 4:
Changes of cytosolic Ca^{2+} with *S*-amlodipine at different concentrations (*S*-amlodipine at 0, 0.1, 0,5, 5, and 10 μmol/L respectively from left to right)

2.2. Effects of (S)-Aml and (R)-Aml on SMC cytosolic Ca^{2+} concentrations

2.2.1. Effects of (S)-Aml on SMC cytosolic Ca^{2+} concentrations

(*S*)-Aml at 0.1 μmol/L, 0.5 μmol/L, 1 μmol/L 5 μmol/L, and 10 μmol/L was applied after normal SMC cytosolic Ca^{2+} was assayed in solution II with 1.8 mmol/L $CaCl_2$ and 40 mmol/L K Cl, $10.3 \pm 1.2\%$, $35.2 \pm 3.5\%$, $60.1 \pm 5.0\%$, $78.9 \pm 6.1\%$, and $91.2 \pm 7.6\%$ cytosolic Ca^{2+} were reduced, respectively ($P < 0.05$, $n = 10$). (*S*)-Aml inhibited SMC cytosolic Ca^{2+} in a concentration-dependent manner (Fig. 4), and IC_{50} was 0.72 ± 0.10 μmol/L.

2.2.2. Effects of (R)-Aml on SMC cytosolic Ca^{2+} concentrations

(*R*)-Aml at 0.1 μmol/L, 0.5 μmol/L, 1 μmol/L, 5 μmol/L, and 10 μmol/L was used after normal cytosolic Ca^{2+} was assayed in solution II with 1.8 mmol/L $CaCl_2$ and 40 mmol/L KCl. However, (*R*)-Aml caused no concentration-dependent inhibition of cytosolic Ca^{2+}, and there was no effect on cytosolic Ca^{2+} at the above concentrations, showing no change of SMC fluorescent signal intensities or ratios.

3. Discussion

Ca^{2+} channels are found in all excitable cells and are essential for electrical excitability, excitation-contraction coupling, excitation-secretion coupling, and other cellular functions. The development of drugs that block Ca^{2+} channels has provided a valuable route for studying channel function, and there is rapidly increasing clinical use of CCBs in combating hypertension, angina, and arrhythmias. Recently, there has been particular interest in the family of dihydropyridine drugs related to Aml (Dahlof et al. 2005; Pathak 2004; Duguay and Deblois 2007; Umemoto et al. 2006).

Aml is a dihydropyride CCB and is widely used for the treatment of cardiovascular diseases (Murdoch ans Heel 1991; Kelly and Malley 1992; Payeras et al. 2007). The high oral bioavailability and long half-life of Aml are unique for this class of drugs and allow safe once-a-day treatment with low doses (Meredith and Elliott 1992). Like most other CCBs of this class, Aml is used therapeutically as a racemate. Many studies have demonstrated that the *R*- and *S*-isomers do not have the same biological activity. Only (*S*)-Aml possesses vasodilatory properties (Pathak et al. 2004; Arrowsmith et al. 1986; Goldmann et al. 1992; Park et al. 2006). However, the underlying mechanism is not well understood, and there has been no report of electrophysiological studies on (*S*)-Aml and (*R*)-Aml, or studies on cytosolic Ca^{2+} changes.

We studied I_{Ca-L} and channel kinetic parameters at different concentrations of (*S*)-Aml and (*R*)-Aml. The results showed that (*S*)-Aml inhibited I_{Ca-L} in a concentration-dependent manner, which illustrated that (*S*)-Aml had the pharmacologic activity associated with CCBs. I_{Ca-L} peak currents were decreased gradually and I–V curves were shifted upward with the increase of (*S*)-Aml concentrations; however, there was no significant change in I–V curve morphology, peak current activation potential, reverse potential or threshold potential. These changes appeared only in I_{Ca-L} and peak current amplitude, but threshold potential and reverse potential were not changed, demonstrating that (*S*)-Aml had effects on only the calcium channel, and not on other channels.

The steady-state activation curve can demonstrate the activation threshold potential of certain ionic channels. In the present study, we found that steady-state activation curves were shifted to the left, and half-activation voltages were decreased with the increase of (*S*)-Aml concentrations, which showed that more negative potential was needed to obtain the same current ratio when the calcium channel was blocked by (*S*)-Aml. On the other hand, the steady-state inactivation curve can show that a certain rest potential is needed when a channel opens. With the increase of (*S*)-Aml concentrations, steady-state inactivation curves were shifted to the left and half-activation voltages were decreased, which also showed that more negative potential was needed to obtain the same current ratio when the calcium channel was blocked by (*S*)-Aml. With the increase of (*S*)-Aml concentrations, time constants of I_{Ca-L} recovery curves from inactivation were prolonged gradually, meaning more time was needed to obtain the same current ratio when the calcium channel was blocked by (*S*)-Aml. However, when (*R*)-Aml was used in different concentrations, it had no effect on I_{Ca-L}, peak currents, I–V curves, steady-state activation curves, steady-state inactivation curves, or recovery curves from inactivation, which showed that (*R*)-Aml had none of the pharmacological actions associated with CCBs, and cannot block calcium channels.

The present study was undertaken to investigate the influences of (*S*)-Aml and (*R*)-Aml on intracellular Ca^{2+} by using the fluorescent probe Fura-2/AM (Guo et al. 2004). After normal cytosolic Ca^{2+} concentrations were assayed with the fluorescent probe Fura-2/AM, (*S*)-Aml and (*R*)-Aml at concentrations of 0.1 μmol/L, 0.5 μmol/L, 1 μmol/L, 5 μmol/L, and 10 μmol/L were utilized. As far as (*S*)-Aml was concerned, fluorescent signal densities and ratios were decreased gradually when it was used at increased concentrations, which showed that (*S*)-Aml could reduce SMC cytosolic Ca^{2+} in a concentration-dependent manner. It can be concluded that (*S*)-Aml blocks voltage-dependent L-type calcium channels, and prevents extracellular Ca^{2+} from entering SMCs. However, there was no significant change in fluorescent signal intensities or fluorescent signal ratios of SMCs when (*R*)-Aml was applied at above concentrations, which demonstrated that there was no change of SMC cytosolic Ca^{2+}, i.e. (*R*)-Aml cannot block L-type calcium channels.

Cell contraction is usually initiated by a transient rise in cytoplasmic Ca^{2+}, but Ca^{2+} may come from the extracellular space via L-type calcium channels or release from the sarcoplasmic reticulum (Hussain and Orchard 1997). To exclude the latter, we found that fluorescent signal intensities and fluorescent signal ratios were not increased when only KCl was used in different concentrations without Ca^{2+} in the extracellular solution; however, fluorescent signal intensities and fluorescent signal ratios were in-

creased when KCl was applied with 1.8 mmol/L Ca^{2+} in the extracellular solution, which demonstrated that the cytosolic Ca^{2+} increase caused by KCl depolarization was mainly due to Ca^{2+} inflow from the extracellular solution, and not from calcium release from SMC sarcoplasmic reticulum.

In summary, using the patch clamp technique and fluorescent assay, the present findings have clearly shown that only (*S*)-Aml has calcium channel blockade activity, while (*R*)-Aml has none of the pharmacologic actions associated with CCBs.

4. Experimental

4.1. Major experimental instruments

The instruments used were: Axopatch 700B patch clamp amplifier (Axon Instruments, USA), D/A and A/D converter (DigiData 1322, Axon Instruments, USA), Pclamp9.0 pulse software (Axon Instruments, USA), MP-285 motorized micromanipulator (Sutter Instruments, USA), IX71 inverted microscope (Olympus, Japan), SA-OLY/2 and DH-35 culture dish heater (Warner Instruments, USA), P-97 micropipette puller (Sutter Instruments, USA). LAMBDA DG-4 (Sutter Instruments, USA), CCD CoolSNAP ES (Photometrics, USA), and MetaFluor (Molecular Devices, USA).

4.2. Cell isolation

Healthy Spraque-Dawley rats, of either sex, age 8–12 weeks and weighing approximately 200 g, were provided by the Experimental Animal Center of Soochow University (Suzhou, China). Animals were anesthetized with pentobarbital sodium intraperitoneally (i.p.), the heart was removed and retrograde perfusion through the aorta was performed as described (Tytgat 1994). Isolated cells were kept at room temperature and used within 24 h; only relaxed, striated, and rod-shaped cells were used. The investigation conformed to the Guide for the Care and Use of Laboratory Animals published by the PRC National Department of Health.

4.3. Reagents, solutions and drugs

The reagents, solutions and drugs used were: hyaluronidase (Sigma, USA), papain (Biosharp, Korea), dithiothreitol (Biosharp, Korea), rat smooth α-actin monoclonal antibody (DakoCytomation, Denmark), Trypan blue (Sigma, USA), streptavidin-biotin complex immunohistochemistry kit (Boshide, China), and DAB color reagent kit (Boshide, China). Solution I (in mmol/L) was NaCl 127, KCl 5.9, $MgCl_2$ 1.2, $CaCl_2$ 2.4, glucose 12, Hepes 10, pH 7.4 adjusted with NaOH. Solution II was solution I without $CaCl_2$. Enzyme I (in mg/mL) was papain 1.75, dithiothreitol 1.75, bovine serum albumin (BSA) 2.5, dissolved in solution II. Enzyme II (in mg/mL) was collagenase I 2.5, hyaluronidase 2.5, BSA 2.5, dissolved in solution II. I_{Ca-L} internal solution (in mmol/L) was CsCl 120, $CaCl_2$ 1, $MgCl_2$ 5, Hepes 10, EGTA 11, glucose 11, Na_2ATP 5, pH 7.3 adjusted with CsOH. I_{Ca-L} external solution was Tyrode's solution (Yazawa et al. 1990). (*S*)-Aml and (*R*)-Aml, with chemical purity 99.5% and optical purity 99.0%, kindly provided by the Tianfeng Pharmacy Company (Jilin, China), were dissolved in absolute alcohol to make 0.5 mmol/L and 5 mmol/L stock solutions, prepared daily and protected from light. Portions of these stock solutions were added to the Tyrode's solution to obtain the desired final concentrations.

4.4. I_{Ca-L} recording and channel kinetic parameters

Whole-cell voltage clamp currents were recorded following the method of Hamill et al. (1981). In brief, recordings were made using an Axopatch 700B patch clamp amplifier. Voltage clamp pulses were generated via an IBM-compatible computer connected to Digidata 1322. Data acquisition and analyses were performed using pCLAMP software. To obtain I_{Ca-L}, 150ms depolarizing pulses in the range −40 mV to +60 mV were applied to the ventricular myocytes every 500 ms in +10 mV increments from −40 mV holding potential (HP). I_{Ca-L} peak currents were recorded by voltage clamp, with 150 ms depolarizing pulse, 0 mV command voltage, and −40 mV HP (see the inset in Fig. 1). I–V curves of I_{Ca-L} were plotted as current densities and each test potential (see the inset in Fig. 3). In each experiment, to obtain steady-state activation curves, 150 ms depolarizing pulses in the range −40 mV to +10 mV were delivered to the cells every 500 ms in +10 mV increments from −40 mV HP. Steady-state inactivation curves were obtained by applying 1 s pre-pulses within the range −60 mV to 20 mV before a test pulse of 0 mV for 150 ms, then back to −60 mV for 2 s. Calcium channel recovery currents from inactivation were recorded with a 150 ms, 0 mV depolarizing pulse, repeated at intervals of 40 ms, 80 ms, 160 ms, 640 ms, and 1280 ms. Time constants of recovery curves from inactivation were calculated by a single-exponential function fit with current ratios (second/first) and time-intervals. In order to reduce the "run-down" phenomenon of I_{Ca-L}, all recordings of I_{Ca-L} and channel kinetic parameters were performed within 5–20 min after rupture of cell membrane.

4.5. Isolation and identification of rat aortic SMCs

Rats were injected with heparin $5U \cdot g^{-1}$ before pentobarbital sodium 50 mg/kg i.p. (Guo et al. 2004). Arteries of the chest and abdomen were isolated, and placed immediately into solution I at 35–37 °C. Extraneous fat and connective tissue were trimmed from the arteries, and endothelial cells of the theca interna were removed with clean cotton buds. After washing three times with solution I at 35–37 °C, isolated arteries were cut into ~1 mm^3 pieces with scissors and placed into enzyme I for digestion at 35–37 °C for 30 ± 5 min. The supernatant was discarded after centrifugation at 1000 rpm and room temperature for 15 min. The pellet was placed into enzyme II and stirred at 35–37 °C for 15 ± 3 min. The supernatant was discarded again after centrifugation at 1000 rpm and room temperature for 15 min. The pellet was washed three times with solution II, triturated about 20 times with a broken-off Pasteur pipette, and then filtered through 200 μm pore size nylon mesh. Cell morphology was observed with an inverted microscope. Trypan blue was applied to test the activity of isolated cells; only those not dyed blue were living cells. Immunohistochemistry was used to identify α-actin of SMCs.

4.6. Assay of SMC cytosolic Ca^{2+}

Following enzyme treatment of SMC preparations, the surface of the bathing solution is frequently covered with debris which readily affects the experiments. The water surface can be cleaned by wiping with lens paper after cells were allowed to sediment for 3–5 min, and then Fura-2/AM was added to a final concentration of 5 μmol/L with gentle agitation to ensure diffusion of Fura-2/AM throughout the solution. The sample was incubated in the dark for 60 ± 15 min at room temperature. Then solution II was used to perfuse the sample at least three times to eliminate any Fura-2/AM left in solution. The Fura-2-loaded SMCs were excited alternately with ultraviolet light of 340 nm and 380 nm wavelengths, and the concentration of cytosolic Ca^{2+} was assayed in one or two SMCs selected under the inverted microscope. Changes of fluorescent signal intensities reflect changes of cytosolic Ca^{2+} concentrations, which can be calculated as (Grynkiewicz et al. 1985; Zsembery et al. 2003; Girard et al. 2002):

$$[Ca^{2+}]_i = \beta^* K_d^* (R - R_{min})/(R_{max} - R) \quad (1)$$

where $[Ca^{2+}]_i$ is the concentration of free cytosolic Ca^{2+}, β is a proportionality factor associated with selected wavelengths, and K_d is the dissociation constant of Fura-2 and Ca^{2+}, which is 224 nmol/L. R is the fluorescent signal intensity ratio under different experimental conditions, R_{max} is the maximal fluorescent signal intensity ratio when 1% (v/v) Triton X-100 is used. R_{min} is the minimal fluorescent signal intensity ratio when 10 mmol/L edetic acid is applied. Normal concentrations of cytosolic Ca^{2+} were assayed in solution II with 1.8 mmol/L $CaCl_2$ and 40 mmol/L KCl.

4.7. Statistical analysis

Continuous variables were expressed as mean ± deviation ($\bar{x} \pm s$). SPSS11.5 (SPSS Inc, Chicago, Illinois, USA) was used for statistical analysis. Comparisons among groups were performed by analysis of variance (ANOVA) and least-significant difference contrast. Control and drug data for individual groups were compared by Paired t-test. $P \leq 0.05$ was considered significant. OriginPro7.5 software (OriginLab, USA) was utilized to calculate the half-inhibited concentration (IC_{50}).

Acknowledgements: This work was supported, in part, by a grant from Project 135 of Important Laboratory, Jiangsu Province, China. The authors thank Mr Chen Xu-jie and Miss Zhou Ling for their assistance in the preparations of this paper.

References

Arrowsmith JE, Camphell F, Cross E et al. (1986) Long-acting dihydropyridine calcium antagonists. 1. 2-Alkoxymethyl derivatives incorporating basic substituents. J Med Chem 29: 1696–1702.

Bojarski J (2002) Stereoselective chromatography of cardiovascular drugs: an update, J Biochem Biophys Methods 54: 197–220.

Dahlof B, Sever PS, Poulter NR et al. Prevention of cardiovascular events with an antihypertensive regimen of amlodipine adding perindopril as required versus atenolol adding bendroflumethiazide as required, in the Anglo-Scandinavian Cardiac Outcomes Trial-Blood Pressure Lowering Arm (ASCOT-BPLA): a multicentre randomised controlled trial. Lancet 366: 895–906.

Duguay D, Deblois D (2007) Differential regulation of Akt, caspases and MAP kinases underlies smooth muscle cell apoptosis during aortic remodelling in SHR treated with amlodipine. Br J Pharmacol 151: 1315–1323.

Formica RN, Friedman AL, Lorber MI, Smith JD, Eisen T, Bia MJ (2006) A randomized trial comparing losartan with amlodipine as initial therapy for hypertension in the early post-transplant period. Nephrol Dial Transplant 21: 1389–1394.

Girard T, Treves S, Censier K, Mueller CR, Zorzato F, Urwyler A (2002) Phenotyping malignant hyperthermia susceptibility by measuring halothane-induced changes in myoplasmic calcium concentration in cultured human skeletal muscle cells. Br J Anaesth 89: 571–579.

Goldmann S, Stoltefuss J, Born L (1992) Determination of the absolute configuration of the active amlodipine enantiomer as (−)-S: a correction. J Med Chem 35: 3341–3344.

Grynkiewicz G, Poenie M, Tsien RY (1985) A new generation of Ca^{2+} indicators with greatly improved fluorescence properties. J Biol Chem 260: 3440–3450.

Guo CY, Wu JY, Wu YB, Zhong MZ, Lu HM (2004) Effects of endothelin-1 on hepatic stellate cell proliferation, collagen synthesis and secretion, intracellular free calcium concentration. World J Gastroenterol 10: 2697–2700.

Hamill OP, Marty A, Neher E, Sakmann B, Sigworth FJ (1981) Improved patch-clamp techniques for high-resolution current recording from cells and cell-free membrane patches. Pflugers Arch 391: 85–100.

Hussain M, Orchard CH (1997) Sarcoplasmic reticulum Ca^{2+} content, L-type Ca^{2+} current and the Ca^{2+} transient in rat myocytes during beta-adrenergic stimulation. J Physiol 505: 385–402.

Kelly JG, Malley KO (1992) Clinical pharmacokinetics of calcium antagonists. An update. Clin Pharmacokinet 22: 416–433.

Meredith PA, Elliott HL (1992) Clinical pharmacokinetics of amlodipine. Clin Pharmacokinet 22: 22–31.

Murdoch D, Heel RC (1991) Amlodipine. A review of its pharmacodynamic and pharmacokinetic properties, and therapeutic use in cardiovascular disease. Drugs 41: 478–505.

Park JY, Kim KA, Park PW, Lee OJ, Ryu JH, Lee GH, Ha MC, Kim JS, Kang SW, Lee KR (2006) Pharmacokinetic and pharmacodynamic characteristics of a new (*S*)-Amlodipine formulation in healthy Korean male subjects: a randomized, open-label, two-period, comparative, crossover study. Clin Ther 28: 1837–1847.

Pathak L, Hiremath, Kerkar PG, Manade VG (2004) Multicentric, clinical trial of (*S*)-Amlodipine 2.5 mg versus Amlodipine 5 mg in the treatment of mild to moderate hypertension–a randomized, double-blind clinical trial. J Assoc Physicians India 52: 197–202.

Pathak LA (2004) Chiral molecules in hypertension: focus on (*S*)-Amlodipine. J Assoc Physicians India 52: 187–188.

Patil PA, Kothekar MA (2006) Development of safer molecules through chirality, Indian J Med Sci 60: 427–437.

Payeras AC, Sladek K, Lembo G, Alberici M (2007) Antihypertensive efficacy and safety of manidipine versus amlodipine in elderly subjects with isolated systolic hypertension: MAISH study. Clin Drug Investig 27: 623–632.

Sever PS, Poulter NR, Elliott WJ, Jonsson MC, Black HR, Sever PS, Poulter NR, Elliott WJ, Jonsson MC, Black HR (2006) Blood pressure reduction is not the only determinant of outcome. Circulation 113: 2754–2774.

Tytgat J (1994) How to isolate cardiac myocytes. Cardiovasc Res 28: 280–283.

Umemoto S, Kawahara S, Hashimoto R, Umeji K, Matsuda S, Tanaka M, Kubo M, Matsuzaki M (2006) Different effects of amlodipine and enalapril on the mitogen-activated protein kinase/extracellular signal-regulated kinase kinase-extracellular signal-regulated kinase pathway for induction of vascular smooth muscle cell differentiation in vivo. Hypertens Res 29: 179–186.

Yazawa K, Kaibara M, Ohara M, Kameyama M (1990) An improved method for isolating cardiac myocytes useful for patch-clamp studies. Jap J Physiol 40: 157–163.

Zanchetti A, Julius S, Kjeldsen S, Zanchetti A, Julius S, Kjeldsen S, McInnes GT, Hua T, Weber M, Laragh JH, Plat F, Battegay E, Calvo-Vargas C, Cieśliński A, Degaute JP, Holwerda NJ, Kobalava J, Pedersen OL, Rudyatmoko FP, Siamopoulos KC, Störset O. (2006) Outcomes in subgroups of hypertensive patients treated with regimens based on valsartan and amlodipine: an analysis of findings from the VALUE trial. J Hypertens 24: 2163–2168.

Zsembery Á, Boyce AT, Liang LH, Peti-Peterdi J, Bell PD, Schwiebert EM (2003) Sustained calcium entry through P_2X nucleotide receptor channels in human airway epithelial cells. J Biol Chem 278: 13398–13408.